


RESEARCH ARTICLE

Open Access



RNA-Seq reveals the existence of a *CDKN1C-E2F1-TP53* axis that is altered in human T-cell lymphoblastic lymphomas

Pilar López-Nieva^{1,2,3†}, Pablo Fernández-Navarro^{4,5†}, Concepción Vaquero-Lorenzo^{1†}, María Villa-Morales^{1,2,3}, Osvaldo Graña-Castro⁶, María Ángeles Cobos-Fernández^{1,2}, José Luis López-Lorenzo², Pilar Llamas², Laura González-Sánchez^{1,2,3}, Isabel Sastre¹, Marina Pollán^{4,5}, Marcos Malumbres⁷, Javier Santos^{1,2,3*} and José Fernández-Piqueras^{1,2,3*} 

Abstract

Background: Precursor T-cell lymphoblastic lymphomas (T-LBL) are rare aggressive hematological malignancies that mainly develop in children. As in other cancers, the loss of cell cycle control plays a prominent role in the pathogenesis in these malignancies that is primarily attributed to loss of *CDKN2A* (encoding protein p16INK4A). However, the impact of the deregulation of other genes such as *CDKN1C*, *E2F1*, and *TP53* remains to be clarified. Interestingly, experiments in mouse models have proven that conditional T-cell specific deletion of *Cdkn1c* gene may induce a differentiation block at the DN3 to DN4 transition, and that the loss of this gene in the absence of *Tp53* led to aggressive thymic lymphomas.

Results: In this manuscript, we demonstrated that the simultaneous deregulation of *CDKN1C*, *E2F1*, and *TP53* genes by epigenetic mechanisms and/or the deregulation of specific microRNAs, together with additional impairing of *TP53* function by the expression of dominant-negative isoforms are common features in primary human T-LBLs.

Conclusions: Previous experimental work in mice revealed that T-cell specific deletion of *Cdkn1c* accelerates lymphomagenesis in the absence of *Tp53*. If, as expected, the consequences of the deregulation of the *CDKN1C-E2F1-TP53* axis were the same as those experimentally demonstrated in mouse models, the disruption of this axis might be useful to predict tumor aggressiveness, and to provide the basis towards the development of potential therapeutic strategies in human T-LBL.

Keywords: T-cell lymphoblastic lymphoma, *CDKN1C-E2F1-TP53* deregulation, Promoter hypermethylation, Deregulation of miRNAs

Background

Precursor T-cell lymphoblastic neoplasms are aggressive haematological malignancies that mainly develop in children (in particular adolescent males) but also in adults. They derive from maturing thymocytes leading to excessive lymphoblastoid cells in the bone marrow and other lymphoid organs. Clinically, T-cell acute lymphoblastic leukaemia (T-ALL) and T-cell lymphoblastic lymphoma

(T-LBL) are two subgroups differing by the extent of bone marrow infiltration. T-ALL manifests with extensive bone marrow and blood affectation, whereas a mass lesion in the thymus/anterior mediastinum with less than 25% of lymphoblasts in the bone marrow characterizes T-LBL [1].

As in other cancers, the loss of cell cycle control plays a prominent role in the pathogenesis of these malignancies that is primarily attributed to loss of *CDKN2A* (which encodes the tumour suppressor protein p16INK4A) and, to a lesser extent, loss of *RB1* or *CDKN1B* (which encodes p27/KIP1 protein) and aberrantly high levels of *CCND2* (encoding cyclin D2) [2].

* Correspondence: javier.santos@uam.es; jfpiqueras@cbm.csic.es

†Equal contributors

¹Department of Cellular Biology and Immunology, Severo Ochoa Molecular Biology Center (CBMSO), CSIC-Madrid Autonomous University, 28049 Madrid, Spain

Full list of author information is available at the end of the article



Downregulation of *CDKN1C* (which encodes p57/KIP2 protein) by promoter hypermethylation has been detected with very low frequency in paediatric T-ALL and more often in adult patients. However, the biological and clinical impact of hypermethylation and/or loss of *CDKN1C* expression remain uncertain [3]. In addition to T-ALL, downregulation of *CDKN1C* has been observed more frequently in a wide variety of human tumours associated with a strengthening of cell proliferation [4, 5].

In addition, numerous studies have reported that *E2F1* overexpression has clinical relevance in many types of cancers [6]. However, to the best of our knowledge, *E2F1* alterations have not been so far implicated in the development of precursor T-cell neoplasms.

Moreover, the gene encoding TP53 protein, a main downstream effector of E2F1, is frequently targeted in human tumours by gene mutations [7, 8]. Apart from the canonical full-length transcript, it should be noted that alternative splicing of *TP53* and the use of alternate promoter might result in multiple transcript variants and isoforms [9] and, interestingly, abnormal expression of *TP53* isoforms has been reported in many cancers as head and neck, acute myeloid leukaemia (AML) and breast tumours [10] but not in T-cell lymphoblastic neoplasms.

The potential nexus between these three genes has been demonstrated in mice. Some authors [11] have shown in mouse models that inactivation of the *Cdkn1c* gene (also termed as *p57^{KIP2}*) results in thymocyte development arrest at DN3 (Double-Negative 3) to DN4 cells transition, due to hyper-activation of the E2f-Tp53 pathway. Furthermore, the loss of *Cdkn1c* accelerates the development of thymic lymphomas in the absence of the *Tp53* gene.

To assess whether the axis *CDKN1C/E2F1/TP53* plays a role in human T-cell lymphoblastic lymphomas, we investigated the mutational status and the expression levels of these three genes using Next-Generation Sequencing (NSG) approaches. Interestingly, RNA-Sequencing analysis revealed reduced levels of *CDKN1C* mRNA in almost all analysed T-LBL samples, which may be accompanied by increased expression of *E2F1* and overexpression of the *TP53* transcript variant encoding the $\Delta 133TP53$ isoform. Deregulation of these genes is executed by epigenetics mechanisms and deregulation of specific miRNAs.

Methods

Human sample collection

Human T-LBL samples separated in an exploratory cohort (8 samples), an extended cohort (10 samples), and four thymuses of human foetus without haematological pathology, were obtained from the Spanish Hospital

Biobanks Network (RetBioH; www.redbiobancos.es). Lymphomas were diagnosed according to World Health Organization Classification of Hematological Malignancies and recommendations from the European childhood lymphoma pathology panel [12, 13] (Additional file 1: Table S1). Institutional review board approval was obtained for these studies (reference CEI:70–1260).

RNA-sequencing

Total RNA was obtained using TriPure Reagent (Roche Applied Science, Indianapolis, IN, USA), following manufacturer's instructions.

Massive sequencing of mRNAs

RNA Integrity Numbers (RIN) were in the range of 7.2–9.8. Image analysis, per-cycle basecalling and quality score assignment were performed with Illumina Real Time Analysis software (Illumina, San Diego, CA). BCL files were converted to FASTQ format with Illumina's Off-Line Basecaller package (Illumina). The resulting directional RNA-seq libraries were sequenced in paired-end format in two different rounds (Illumina HiSeq2000), leading to 50 bp and 76 bp reads (the latter were trimmed to 50 bp). Sequenced reads were quality-checked with FastQC (<http://www.bioinformatics.babraham.ac.uk/projects/fastqc/>). RNA-seq reads were aligned to the human genome (GRCh37/hg19) with TopHat-2.0.10 [14] (using Bowtie 1.0.0 [15] and Samtools 0.1.19 [16]) allowing two mismatches and five multihits. Transcripts assemblies, estimation of their abundances were calculated with Cufflinks 2.2.1, using the Ensembl GRCh37.74 annotation for human. In this analysis, we only considered the transcripts isoforms of the genes *CDKN1C*, *E2F1* and *TP53* that encode for proteins according to the information showed in Ensembl [17].

Small RNA

Image analysis and per-cycle basecalling was performed with Illumina Real Time Analysis software (RTA1.9) (Illumina). Conversion to FASTQ read format was performed by CASAVA-1.8 (Illumina). Small-RNA-seq libraries were sequenced as 40 bp single-end reads (Illumina Genome Analyzer IIx, GAIIx). Sequenced reads were quality-checked with FastQC. Sequence adapters were removed with cutadapt v1.2.1 [18] and only those reads longer than 15 bp and shorter than 35 bp were kept for further analysis. Reads were aligned to the human genome (GRCh37/hg19) with Bowtie 1.0.0 [15] and Samtools 0.1.19 [16] allowing no mismatches and a maximum of one alignment per read. Raw counts for miRNAs were obtained with HTSeq v0.5.3p9 [19], using the miRBase v20 [20] annotation for hg19. A table with normalized read counts was generated with DESeq [21] and was used to filter out miRNAs with

questionable expression and outliers. The following criteria were used: first, we required that a miRNA should have a minimal normalized count value of 15 in at least 5% of the samples. Second, miRNAs with normalized expression values across the samples that exceeded $Q1 - 3 * IQR$ or $Q3 + 3 * IQR$ were considered outliers and discarded. For the remaining miRNAs, log₂ fold-changes of expression were calculated.

Raw sequencing data and transcripts expression quantification is available as a superseries in GEO (Gene Expression Omnibus) under the following ID: GSE109234.

Additional criteria to select miRNAs

To select those miRNA controlling *CDKN1C*, *E2F1* and *TP53* genes, we used the databases of miRGate and miRTarBase. We select those miRNAs experimentally validated (“Functional miRNA-target interactions (MTI)” registered in “Support type” of miRTarBase and/or “Functional MTI” registered in the miRGate “Confirmed predictions”) and/or those microRNA that showed a “miRGate Agreement Score” equal or higher than the median agreement-value of the microRNA identified associated with the genes assessed (median value = 1.04). (Additional file 2: Figure S1).

Additionally, we filtered out miRNAs showing a number of counts lower than 28.70 (median value of the miRNA counts of all the samples) in any sample (Additional file 3: Figure S2).

Quantitative RT-PCR

RNA was reverse-transcribed using first the High-Capacity RNA-to-cDNA™ Kit (Applied Biosystems, Foster City, CA, USA) and MystiCq microRNA cDNA Synthesis Mix (Sigma-Aldrich, St. Louis, MO, USA). Quantitative real-time PCR reactions were performed in triplicate with an Applied Biosystems 7300 Real-Time PCR system (Life Technologies, Carlsbad, CA), using either the Fast Start Universal SYBRGreen Master (Rox) (Roche) or the MystiCq microRNA SYBR Green qPCR ReadyMix (Sigma-Aldrich), according to the manufacturers’ instructions. Expression values of β -2-microglobulin or β -actin or SNORD48 served to normalize using the $2^{-\Delta\Delta C_T}$ method [22]. Primers are indicated in Additional file 4: Table S2.

Targeted gene deep sequencing and sanger sequencing

Mutational status of *CDKN1C*, *E2F1* and *TP53* genes was analysed by targeted deep sequencing in genomic using a selected panel of cancer-related genes (the OncoNIM® Seq409 panel; New Integrated Medical genetics; NIMGenetics, Madrid, Spain). Sanger DNA sequencing of PCR-amplified mutational hot spots was performed with the specific primers summarized in Additional file 4: Table S2.

Bisulfite genomic sequencing and methylation-specific PCR (MSP)

Methyl Primer Express v1.0 software (Applied Biosystems) was used to identify CpG islands around the Transcriptional Start Site (TSS) of *CDKN1C* gene, and to design specific primers for the methylation analysis. DNA (1 μ g) was subjected to sodium bisulfite treatment using the EZ DNA Methylation-Gold kit (Zymo Research, CA, USA). MSP was performed with primers specific for methylated (M) or unmethylated (U) CpG sites. For bisulfite genomic sequencing, a region included in the one analysed by MSP was amplified using 1 μ L of bisulfite-converted DNA with Immolase Taq polymerase (Bioline USA Inc., Kenilworth, NJ) at 60 °C for 40 cycles. Then the resulting PCR products were gel-purified (2% agarose) with Wizard® SV Gel and PCR Clean-Up System (Promega, Madison, WI, USA) and cloned into the pGEMT Easy Vector System (Promega) following the manufacturer-specific protocols. For all samples, 12 colonies were randomly chosen, and DNA was purified using Wizard® Plus SV Minipreps DNA Purification System (Promega) and sequenced with a ABI 3730 xl DNA Analyzer (Applied Biosystems). After sequencing analysis, the results were transformed into percentages of CpGs calculated in comparison with the total CpGs of the analysed region. Primers and conditions are indicated in Additional file 4: Table S2.

Statistical analyses

Differential expression of mRNA and miRNA (RNA-Seq) between tumours and controls was estimated by calculating the log₂ Fold changes (log₂FC) of the expression levels. Only differential expression levels estimated by the Cufflinks software as “OK” were taken into account. Significant deregulated miRNAs with log₂FC absolute values equal or higher than 1.5 in at least in one sample were selected according to the information of miRGate and miRTarBase databases [23, 24] and additional criteria based on the read counts [25]. Student’s t-test was used to compare results from qRT-PCR between tumours and controls. All statistical analyses were performed using R software.

Results

Deregulation of *CDKN1C*, *E2F1* and *TP53* in T-LBLs

The results of massive RNA-sequencing (RNA-Seq) of the transcript isoforms that encode proteins in the 8 T-LBL samples of the exploratory cohort showed that the mRNA level of *CDKN1C* was strongly reduced in all analysed tumours compared to that of the normal foetal thymuses, with fold-changes ranging from - 25.99 to - 2.15 in the canonical isoform ENST00000414822. By contrary, the expression of *E2F1* gene in the same panel increases in all tumours, three of them with fold-changes higher than 1.5. Concerning the transcriptional

status of the *TP53* gene, we found increased levels of the transcript variant encoding the dominant-negative $\Delta 133p53\alpha$ protein isoform (TP53–008: ENST00000504937) in all but two of the eight tumours (fold-changes between 3.26 and 0.74). Moreover, two of them (346 and 460) exhibited a clear reduction of two transcript variants (TP53–001: ENST00000269305 and TP53–002: ENST00000445888) encoding full-length TP53 protein isoforms (TAp53 α). Finally, two tumours (192 and 521) showed increased amounts of the TP53 β transcript (ENST00000420246), which encodes a C-terminal truncated protein (Figs. 1 and 2; Additional file 5: Table S3).

These results were validated by quantitative real-time RT-PCR (qRT-PCR) analysis and confirmed in the extended cohort (Fig. 3; Additional file 6: Table S4). Interestingly, all samples in the extended cohort showed a significant reduction of *CDKN1C* expression, six out of ten showed significant increases of *E2F1* expression, and six out of ten exhibited significant increases of the mRNA isoform encoding $\Delta 133p53\alpha$ protein.

Overrepresentation of the arginine allele at codon 72 of TP53 in T-LBLs

The analysis of T-LBLs by targeted gene deep sequencing revealed the existence of two missense mutations. One of them was c.427G > T (p.Val143Leu) at exon 5 in sample 192, with conflicting interpretations of pathogenicity in the IARC database [26]. The other missense

mutation was the functional polymorphism c.215C > G (p.Pro72Arg) that was found in all but one analysed tumours (8/9), three of them being homozygotes for the arginine allele (238, 521, and 840) (Additional file 7: Table S5) (Fig. 2). However, we were able to validate only the mutation at exon 4 by DNA Sanger-sequencing (data not shown) using the primers and conditions indicated in Additional file 4: Table S2.

Epigenetic modifications contribute to the altered expression of CDKN1C in a fraction of T-LBLs

The *CDKN1C* gene is remarkably rich in CpG islands situated both upstream and downstream from the transcriptional start site, whose hypermethylation has been strongly related to its inactivation [27]. To elucidate whether aberrant DNA methylation is a mechanism whereby *CDKN1C* was downregulated in our T-LBLs, we analysed the DNA methylation levels of the promoter region of *CDKN1C* gene using the MSP/Sequencing method. We initially examined six samples of normal foetal thymuses by MSP, confirming the absence of methylated bands in all cases (data not shown). However, although all samples in the exploratory cohort exhibited significant downregulation of this gene, only two tumours exhibited high levels of hypermethylation (521 and 840), suggesting additional mechanisms to explain *CDKN1C* downregulation in the remaining samples (Fig. 4).

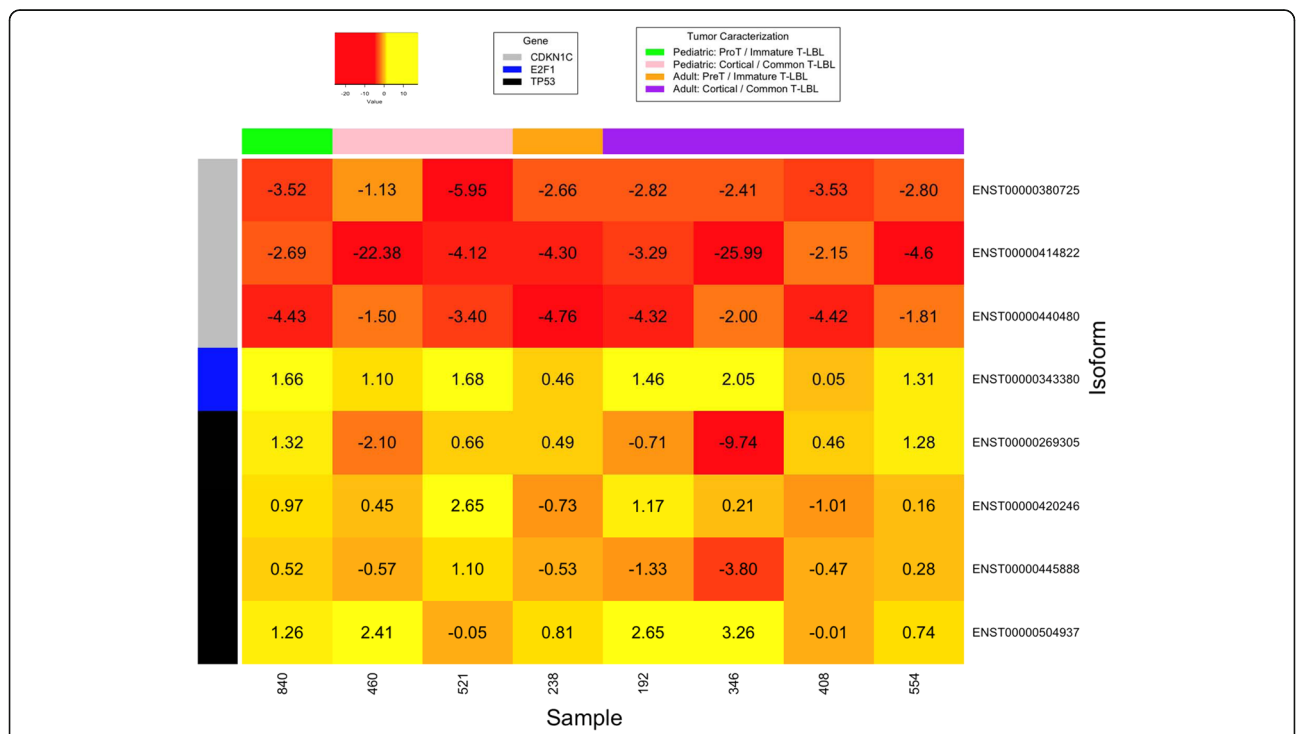


Fig. 1 Deregulation of *CDKN1C*, *E2F1* and *TP53* in T-LBLs of the exploratory cohort by RNA-Seq. Numbers indicate log2 Fold changes (log2FC) between the expression of mRNAs in tumours and controls. Positive and negative values represent overexpression and reduced expression, respectively

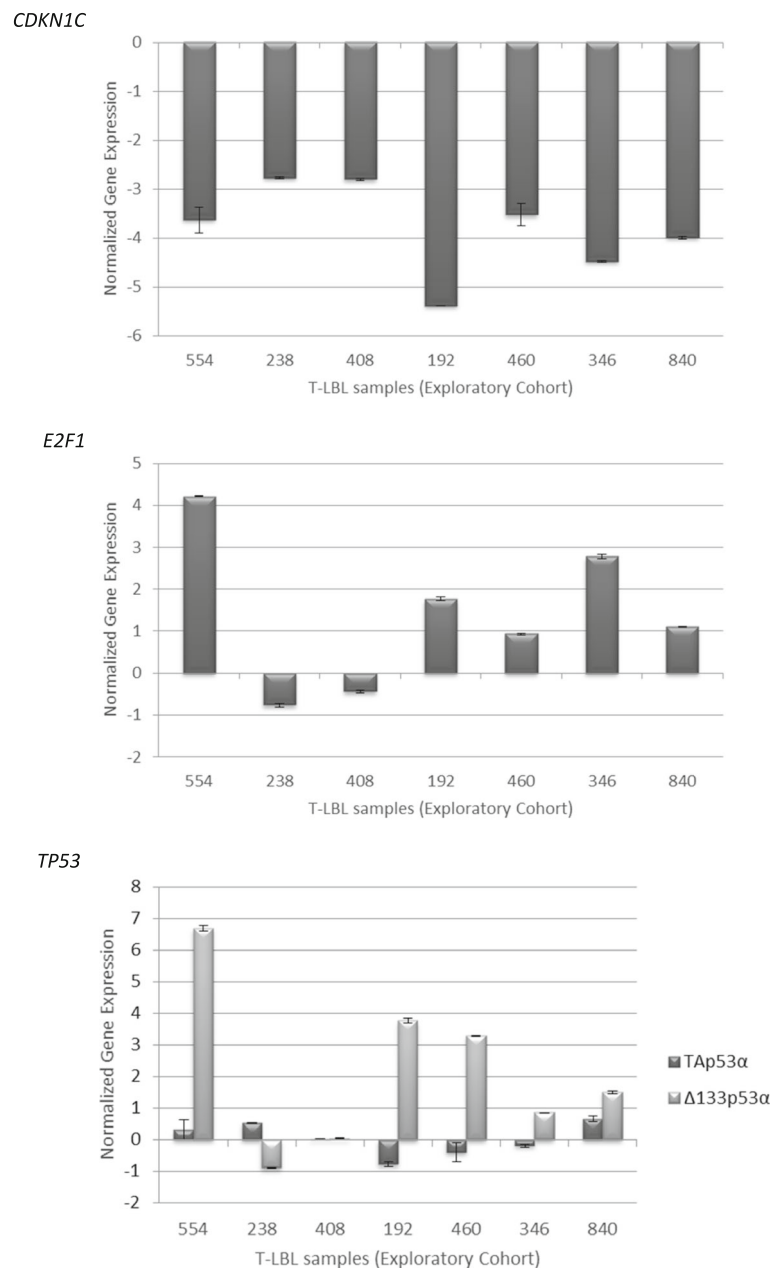


Fig. 3 Differential expression of *CDKN1C*, *E2F1* and *TP53* in T-LBLs of the exploratory cohort by quantitative RT-PCR. Relative expression values were calculated as the mRNA amount of each gene relative to that of either β -actin or $\beta 2$ microglobulin (used as reference) and normalized to the relative expression of normal control samples (foetal thymuses). Each bar represents the mean \pm SD of three independent experiments. Differences in expression values were statistically significant ($p < 0.05$)

Methylated Region 1 (KvDMR1) in the promoter of the noncoding *KCNQ1OT1* [37, 38]. Although the biological and clinical impact of *CDKN1C* hypermethylation is rather uncertain, aberrant DNA methylation of *CDKN1C* in its promoter region has been reported in lymphoid malignancies of B and T-cell phenotype [39, 40]. However, *CDKN1C* has been reported downregulated in other type of cancer cells mainly by histone modifications operating in critical regions of its promoter [41, 42]. We initially

focused on promoter hypermethylation to explain downregulation of this gene in our sample series of T-LBL, but despite a substantial reduction in the levels of mRNA in almost all samples in the exploratory cohort (7/8), only two samples (840 and 521) (2/8) exhibited significant hypermethylation density (Fig. 4), and six out of eight (including tumor 840 with promoter hypermethylation) exhibited upregulation of one or two miRNAs selected for *CDKN1C* regulation (miR-211-3p and miR-222-3p).

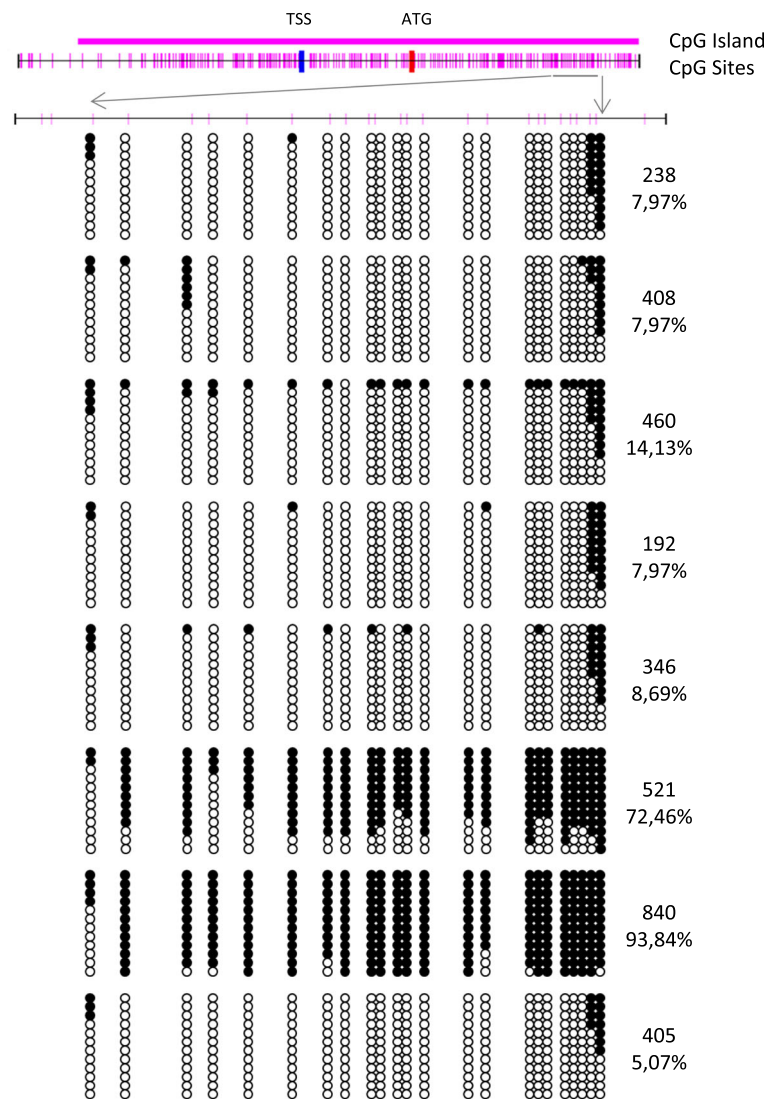


Fig. 4 Schematic depiction of the CpG-island around the transcription start site of *CDKN1C* (TSS). ATG indicate the position of the translation start site. Short vertical lines represent CpG dinucleotides. Methylated (black circles) or unmethylated (white circles) CpG sites are indicated in 12 sequenced clones for every tumour. Methylation density is indicated as the percentage of methylated sites in comparison with total CpG sites

Thus, downregulation of *CDKN1C* in two samples (33 and 346) should be explained by a different transcriptional mechanism.

Besides this epigenetic mechanism, regulation by miRNAs might be an additional way contributing to determine *CDKN1C* transcript levels in T-LBLs. Results reported here are in line with those reported in the literature describing miR-25, miR-221 and miR-222 as direct regulators of *CDKN1C* expression in a wide variety of solid tumours, showing a new mechanism responsible for *CDKN1C* downregulation in carcinogenesis [43–45]. In this context, our findings suggest that aberrant expression of miR-221 and miR-222 may have an oncogenic function in T-LBL development by targeting *CDKN1C*. However two samples (33 and 346) showed a

pronounced downregulation of *CDKN1C* in the absence of significant changes in miRNA expression (Figs. 5 and 6) or promoter CpG methylation, thus indicating that the mechanism regulating the expression of this gene is far more complex.

Overexpression of *E2F1* may promote proliferation or cell cycle progression by increasing the transcription of genes that contribute to G1-S transition [46]. Notwithstanding at the same time it may also induce apoptosis by multiple pathways, some of which induce stabilization and activation of the TP53 protein [47]. Our microRNA analysis also revealed a consistent deregulation of seven miRNAs in T-LBLs, miR-203a and miR-205-5p being the most representative downregulated microRNAs (Figs. 5 and 6). Interestingly, downregulated miRNAs

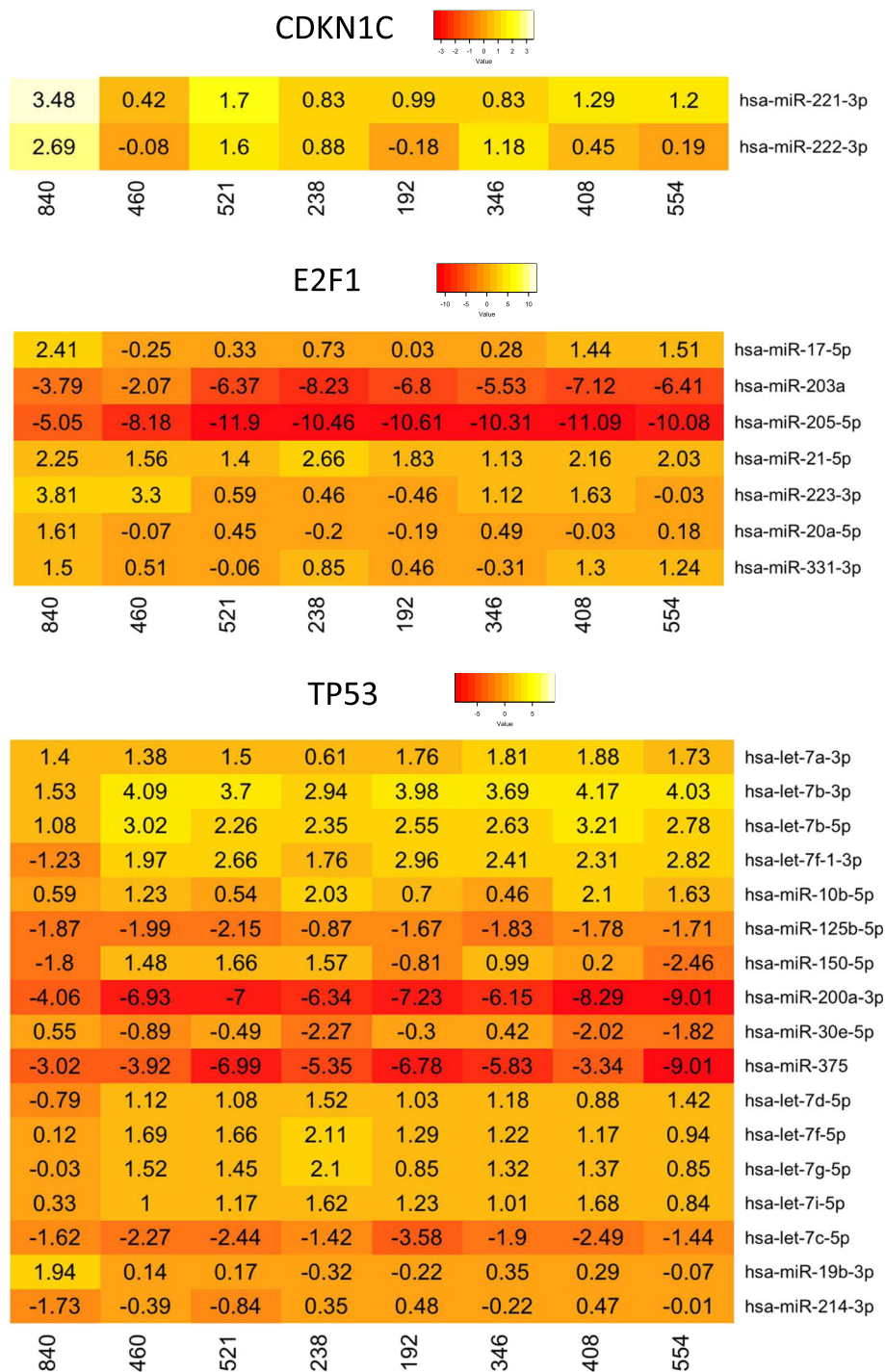


Fig. 5 Deregulated MicroRNA controlling *CDKN1C*, *E2F1* and *TP53* genes in T-LBLs of the exploratory cohort (RNA-Seq). Numbers indicate log2 Fold changes (log2FC) between the miRNAs read counts in tumours and controls. Positive and negative values represent up-regulated and down-regulated, respectively. Only miRNAs showing log2FC absolute values equal or higher than 1.5 in at least in one sample are depicted. The number in each column represents the sample identifier

showed higher fold changes than upregulated microRNAs. miR-205-5p is known to be down-regulated in melanoma and its expression inversely correlated with that of *E2F1* [48].

Concerning impairing of *TP53* function, we found overexpression of the human *Δ133p53* isoform in 4 samples from the exploratory cohort, from which three also exhibited downregulation of the isoform encoding

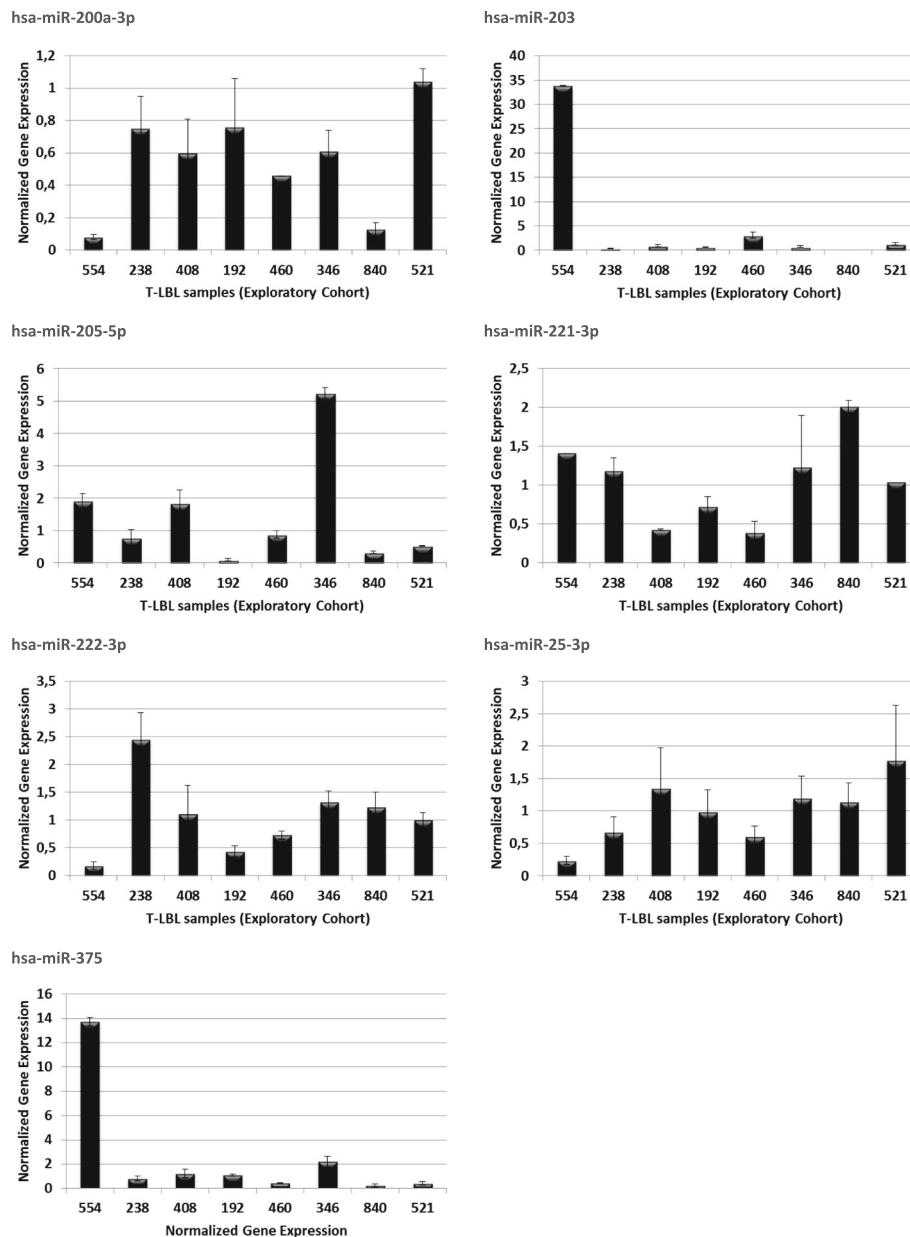
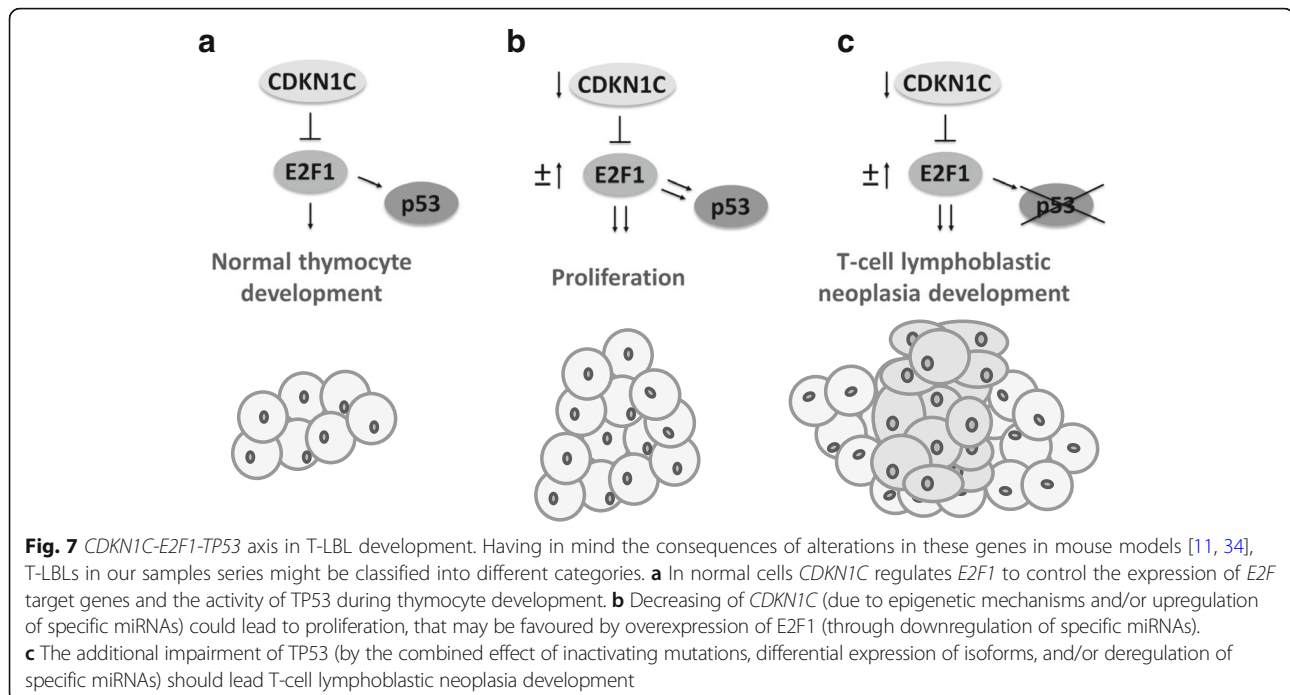


Fig. 6 Differential expression of miRNAs regulating *CDKN1C*, *E2F1* and *TP53* expression by interaction with its 3'UTR. Transcriptional levels of hsa-miR-200a-3p, hsa-miR-203, hsa-miR-205-5p, hsa-miR-221-3p, hsa-miR-222-3p, hsa-miR-25-3p and in human T-LBLs were measured using qRT-PCR assay. Relative expression values were calculated as the mRNA amount of each gene relative to miR-SNORD48 (used as reference) and normalized to the relative expression of normal control samples (foetal thymuses). Each bar represents the mean \pm SD of three independent experiments. Differences in expression values were statistically significant ($p < 0.05$)

full length *TP53* protein isoforms (Figs. 1 and 2). It has been demonstrated that $\Delta 133p53\alpha$ does not exclusively function in a dominant-negative manner toward *TP53*, the full-length *TP53* isoform [49], but it also inhibits *TP53*-dependent apoptosis [50]. Finally, two tumours (192 and 521) showed increased amounts of the *TP53* β transcript, which encodes a C-terminal truncated protein that downplay *TP53* capacity to induce apoptosis [9, 51]. These changes in the expression levels of full

length and shorter isoforms may be sustained, at least in part, by deregulation of 17 miRNAs, with particular reference to miR-200a-3p and miR-375 that exhibited very high levels of downregulation in all samples in the exploratory cohort (Figs. 5 and 6).

But impairment of the *TP53* function could be also attributed to the overrepresentation of the arg72 allele in our sample series (Fig. 2). It is known that the *TP53* gene is not only frequently mutated in human tumours



[7], but it also contains several functional polymorphisms, being by far the most common a proline (Pro) to arginine (Arg) change at codon 72 in the TP53 protein [10]. Several studies have reported preferential retention of arg72 allele in squamous cell carcinomas of the vulva [52], head and neck [53], and esophagus [54]. Considering tumour tissue DNA, Schneider-Stock et al. [55] found a significantly higher frequency of the arg72 allele in colorectal tumours and reported that the presence of this allele correlates with the malignant potential of the tumour. Similar results were also reported in urinary tract cancers [56] and lung cancer [57]. The arg72 allele was also related with increased risk for bladder cancer [58].

Conclusions

Our results indicate the existence of a *CDKN1C-E2F1-TP53* axis that is disrupted in a significant fraction of human T-LBLs. If, as expected, the consequences of the deregulation of the *CDKN1C-E2F1-TP53* axis were the same as those experimentally demonstrated in mouse models, deregulation of this axis in human T-LBL might serve as a biomarker to predict the aggressiveness of T-LBL development as depicted in Fig. 7. Furthermore, these findings would provide the basis to the development of potential therapeutic strategies based on the use of microRNAs (mimics or antagomirs) to target *CDKN1C* or *E2F1* deregulation that allow to rescue normal thymocyte differentiation and normal levels of thymocytes proliferation in patients with T-LBL. Blocking *E2F1* expression by RNA interference might

represent a promising therapeutic approach in this type of tumours. Future studies with new samples series of T-LBL should be done to be sure that the differences detected at the mRNA level translate into the protein level, and to confirm that the deregulation of this axis in human samples is really predictive of clinical outcome.

Additional files

- Additional file 1: Table S1.** Characterization of the human sample collection in the exploratory cohort. Lymphomas were diagnosed (see Characterization column) according to World Health Organization Classification of Hematological Malignancies and recommendations from the European. (PDF 205 kb)
- Additional file 2: Figure S1.** Gaussian Kernel Density plot of miRGate Agreement Score of the miRNAs identified associated with the *CDKN1C*, *E2F1* and *TP53* genes. (PDF 283 kb)
- Additional file 3: Figure S2.** Gaussian Kernel Density Plot of the red counts for the miRNAs deregulated in any sample. (PDF 1208 kb)
- Additional file 4: Table S2.** Description of primers used in qRT-PCR, Targeted gene deep sequencing, Sanger sequencing and Methylation-Specific PCR. (PDF 95 kb)
- Additional file 5: Table S3.** Differential expression of mRNA between tumours and controls in the exploratory cohort by RNA-Seq. (PDF 77 kb)
- Additional file 6: Table S4.** Relative expression of *CDKN1C*, *E2F1* and *TP53* analyzed by qRT-PCR. (PDF 88 kb)
- Additional file 7: Table S5.** Complete list of genetic variants for *TP53* gene determined by targeted deep sequencing in the T-LBL samples. (PDF 96 kb)
- Additional file 8: Table S6.** MicroRNA regulation of *CDKN1C*, *E2F1* and *TP53* genes in T-LBLs of the exploratory cohort by RNA-Seq. (PDF 78 kb)
- Additional file 9: Table S7.** Validation analysis by qRT-PCR of those miRNA significantly deregulated according with RNA-Seq analysis in the exploratory and extended cohort of T-LBL samples. (PDF 81 kb)

Abbreviations

AML: Acute myeloid leukaemia; DN3: Double-Negative 3; DN4: Double-Negative 4; FC: Fold-change; FDR: False discovery rate; GEO: Gene Expression Omnibus; KvDMR1: Kv-Differentially Methylated Region 1; miRNAs: microRNAs; MTI: miRNA-target interactions; NSG: Next-Generation Sequencing; qRT-PCR: Quantitative reverse transcription polymerase chain reaction; RIN: RNA Integrity Numbers; RNA-Seq: Massive RNA-sequencing; RT-PCR: Reverse transcription polymerase chain reaction; T-ALL: T-cell acute lymphoblastic leukaemia; T-LBL: T-cell lymphoblastic lymphomas

Acknowledgements

The authors would like to thank Mario González-Sánchez and Javier González-Palacios ("Bioinformatics and Research Group in Genetic and Environmental Epidemiology", ISCIII) for their technical support. We thank all patients who were willing to donate their samples—without their support the research work would not be possible.

Funding

The authors would like to thank the Spanish Ministry of Economy and Competitiveness (SAF2015–70561-R; MINECO/FEDER, EU) and the Autonomous Community of Madrid, Spain (B2017/BMD-3778; LINFOMAS-CM) for funding this work. Institutional grants from the Fundación Ramón Areces and Banco de Santander are also acknowledged. ORCID codes: 0000–0003–4520–6785 to JFP and 0000–0002–4168–6251 to JS. The funding body did not play any role in the study design, collection, analysis, and interpretation of data and in writing the manuscript.

Availability of data and materials

Raw sequencing data and transcripts expression quantification is available as a superseries in GEO (Gene Expression Omnibus) under the following ID: GSE109234. The remaining datasets supporting the conclusions of this article are included within the article and its Additional files.

Authors' contributions

PLN, PFN and CVL developed the concepts, designed the experiments and contributed to the writing of the manuscript. PLN performed epigenetic experiments and analysis. PLN and CVL quantified gene expression. PFN conducted all the bioinformatics analyses. MVM, MACF, LGS and IS performed experiments. OGC, JLLL, PLI, MP and MM all read and revising the final manuscript critically. JF and JS directed the study, analyzed the results and wrote the manuscript. All authors have read and approved the final manuscript.

Ethics approval and consent to participate

The study was conducted in accordance with the Declaration of Helsinki and the Spanish legislation for the use of archived tissue specimens and associated clinical information. The clinical data were retrieved, and the histological samples were collected and analysed with the endorsement of the Madrid Autonomous University Research Ethics Committee (reference CEI: 70–1260). All the specimens were from Spanish Hospital Biobanks Network (RetBioH; www.redbiobancos.es). Biobanks authorized and inspected by National Supervisory Authority for Welfare and Health can provide human specimens collected during diagnostic procedures and associated clinical information for research purposes based on the biobank's scientific board review. Personal data will be collected, processed and stored adhering at all times to the obligation of maintaining confidentiality, in accordance with current legislation regarding the protection of personal data (Informed consent form: http://www.redbiobancos.es/DownloadHandler.ashx?f=HIP_CI_RNBB_2012_aprobado_ING.pdf&s=-1&p=-1&d=319). Identification of the biological samples of the Biobank will be subjected to a coding process. Each sample is assigned an identification code. Lymphomas were diagnosed according to World Health Organization Classification of Hematological Malignancies and recommendations from the European childhood lymphoma pathology panel.

Consent for publication

Not applicable.

Competing interests

The authors declare that they have no competing interests.

Publisher's Note

Springer Nature remains neutral with regard to jurisdictional claims in published maps and institutional affiliations.

Author details

¹Department of Cellular Biology and Immunology, Severo Ochoa Molecular Biology Center (CBMSO), CSIC-Madrid Autonomous University, 28049 Madrid, Spain. ²Institute of Health Research, Jiménez Díaz Foundation, Madrid, Spain. ³Consortium for Biomedical Research in Rare Diseases (CIBERER), Carlos III Institute of Health, Madrid, Spain. ⁴Cancer and Environmental Epidemiology Unit, National Center for Epidemiology, Carlos III Institute of Health, Madrid, Spain. ⁵Consortium for Biomedical Research in Epidemiology and Public Health (CIBERESP), Madrid, Spain. ⁶Bioinformatics Unit, Structural Biology and Biocomputing Programme, Spanish National Cancer Research Center (CNIO), Madrid, Spain. ⁷Cell Division and Cancer Group, Molecular Oncology Programme, Spanish National Cancer Research Centre (CNIO), Madrid, Spain.

Received: 26 June 2017 Accepted: 26 March 2018

Published online: 16 April 2018

References

- de Leval L, Bisig B, Thielen C, Boniver J, Gaulard P. Molecular classification of T-cell lymphomas. *Crit Rev Oncol Hematol*. 2009;72(2):125–43.
- Belver L, Ferrando A. The genetics and mechanisms of T cell acute lymphoblastic leukaemia. *Nat Rev Cancer*. 2016;16(8):494–507.
- Bonn BR, Krieger D, Burkhardt B. Cell cycle regulatory molecular profiles of pediatric T-cell lymphoblastic leukemia and lymphoma. *Leuk Lymphoma*. 2012;53(4):557–68.
- Besson A, Dowdy SF, Roberts JM. CDK inhibitors: cell cycle regulators and beyond. *Dev Cell*. 2008;14(2):159–69.
- Guo H, Lv Y, Tian T, Hu TH, Wang WJ, Sui X, Jiang L, Ruan ZP, Nan KJ. Downregulation of p57 accelerates the growth and invasion of hepatocellular carcinoma. *Carcinogenesis*. 2011;32(12):1897–904.
- Chen HZ, Tsai SY, Leone G. Emerging roles of E2Fs in cancer: an exit from cell cycle control. *Nat Rev Cancer*. 2009;9(11):785–97.
- Olivier M, Hollstein M, Hainaut P. TP53 mutations in human cancers: origins, consequences, and clinical use. *Cold Spring Harb Perspect Biol*. 2010;2(1):a001008.
- Liontos M, Niforou K, Velimezi G, Vougas K, Evangelou K, Apostolopoulou K, Vrtel R, Damalas A, Kontovazenis P, Kotsinas A, et al. Modulation of the E2F1-driven cancer cell fate by the DNA damage response machinery and potential novel E2F1 targets in osteosarcomas. *Am J Pathol*. 2009;175(11):376–91.
- Khoury MP, Bourdon JC. The isoforms of the p53 protein. *Cold Spring Harb Perspect Biol*. 2010;2(3):a000927.
- Bourdon JC. p53 and its isoforms in cancer. *Br J Cancer*. 2007;97(3):277–82.
- Matsumoto A, Takeishi S, Nakayama KI. p57 regulates T-cell development and prevents lymphomagenesis by balancing p53 activity and pre-TCR signaling. *Blood*. 2014;123(22):3429–39.
- Oschlies I, Burkhardt B, Chassagne-Clement C, d'Amore ES, Hansson U, Hebeda K, Mc Carthy K, Kodet R, Malydk J, Mullauer L, et al. Diagnosis and immunophenotype of 188 pediatric lymphoblastic lymphomas treated within a randomized prospective trial: experiences and preliminary recommendations from the European childhood lymphoma pathology panel. *Am J Surg Pathol*. 2011;35(6):836–44.
- WHO Classification of Tumours of Haematopoietic and Lymphoid Tissues. WHO Classification of Tumours, 4th Edition, Volume 2. Edited by Swerdlow SH, Campo E, Harris NL, Jaffe ES, Pileri SA, Stein H, Thiele J, Vardiman JW. IARC (International Agency for Research on Cancer) publications; 2008.
- Trapnell C, Roberts A, Goff L, Pertea G, Kim D, Kelley DR, Pimentel H, Salzberg SL, Rinn JL, Pachter L. Differential gene and transcript expression analysis of RNA-seq experiments with TopHat and cufflinks. *Nat Protoc*. 2012;7(3):562–78.
- Langmead B, Trapnell C, Pop M, Salzberg SL. Ultrafast and memory-efficient alignment of short DNA sequences to the human genome. *Genome Biol*. 2009;10(3):R25.
- Li H, Handsaker B, Wysoker A, Fennell T, Ruan J, Homer N, Marth G, Abecasis G, Durbin R. The sequence alignment/map format and SAMtools. *Bioinformatics*. 2009;25(16):2078–9.
- Yates A, Akanni W, Amode MR, Barrell D, Billis K, Carvalho-Silva D, Cummins C, Clapham P, Fitzgerald S, Gil L, et al. Ensembl 2016. *Nucleic Acids Res*. 2016;44(D1):D710–6.

18. Martin M. Cutadapt removes adapter sequences from high-throughput sequencing reads. *EMBnet J.* 2011;17(1):3.
19. Anders S, Pyl PT, Huber W. HTSeq—a Python framework to work with high-throughput sequencing data. *Bioinformatics.* 2015;31(2):166–9.
20. Kozomara A, Griffiths-Jones S. miRBase: annotating high confidence microRNAs using deep sequencing data. *Nucleic Acids Res.* 2014; 42(Database issue):D68–73.
21. Anders S, McCarthy DJ, Chen Y, Okoniewski M, Smyth GK, Huber W, Robinson MD. Count-based differential expression analysis of RNA sequencing data using R and Bioconductor. *Nat Protoc.* 2013;8(9):1765–86.
22. Livak KJ, Schmittgen TD. Analysis of relative gene expression data using real-time quantitative PCR and the 2^{−(ΔΔC_T)} method. *Methods.* 2001;25(4):402–8.
23. Chou CH, Chang NW, Shrestha S, Hsu SD, Lin YL, Lee WH, Yang CD, Hong HC, Wei TY, Tu SJ, et al. miRTarBase 2016: updates to the experimentally validated miRNA-target interactions database. *Nucleic Acids Res.* 2016; 44(D1):D239–47.
24. Andres-Leon E, Gonzalez Pena D, Gomez-Lopez G, Pisano DG. miRGate: a curated database of human, mouse and rat miRNA-mRNA targets. *Database (Oxford).* 2015;2015:bav035.
25. Mullokandov G, Baccarini A, Ruzo A, Jayaprakash AD, Tung N, Israelow B, Evans MJ, Sachidanandam R, Brown BD. High-throughput assessment of microRNA activity and function using microRNA sensor and decoy libraries. *Nat Methods.* 2012;9(8):840–6.
26. Bouaoun L, Sonkin D, Ardin M, Hollstein M, Byrnes G, Zavadil J, Olivier M. TP53 variations in human cancers: new lessons from the IARC TP53 database and genomics data. *Hum Mutat.* 2016;37(9):865–76.
27. Matsuoka S, Thompson JS, Edwards MC, Bartletta JM, Grundy P, Kalikin LM, Harper JW, Elledge SJ, Feinberg AP. Imprinting of the gene encoding a human cyclin-dependent kinase inhibitor, p57KIP2, on chromosome 11p15. *Proc Natl Acad Sci U S A.* 1996;93(7):3026–30.
28. Negrini M, Ferracin M, Sabbioni S, Croce CM. MicroRNAs in human cancer: from research to therapy. *J Cell Sci.* 2007;120(Pt 11):1833–40.
29. Bueno MJ, Malumbres M. MicroRNAs and the cell cycle. *Biochim Biophys Acta.* 2011;1812(5):592–601.
30. Jin RJ, Lho Y, Wang Y, Ao M, Revelo MP, Hayward SW, Wills ML, Logan SK, Zhang P, Matusik RJ. Down-regulation of p57Kip2 induces prostate cancer in the mouse. *Cancer Res.* 2008;68(10):3601–8.
31. Schwarze SR, Shi Y, Fu VX, Watson PA, Jarrard DF. Role of cyclin-dependent kinase inhibitors in the growth arrest at senescence in human prostate epithelial and uroepithelial cells. *Oncogene.* 2001;20(57):8184–92.
32. Lu L, Qiu J, Liu S, Luo W. Vitamin D3 analogue EB1089 inhibits the proliferation of human laryngeal squamous carcinoma cells via p57. *Mol Cancer Ther.* 2008;7(5):1268–74.
33. Dos Reis VL, Pujiz RS, Strauss BE, Krieger JE. Knockdown of E2f1 by RNA interference impairs proliferation of rat cells in vitro. *Genet Mol Biol.* 2010; 33(1):17–22.
34. Jayapal SR, Kaldis P. p57(Kip2) regulates T-cell development and lymphoma. *Blood.* 2014;123(22):3370–1.
35. de Sousa AR, Penalva LO, Marcotte EM, Vogel C. Global signatures of protein and mRNA expression levels. *Mol Biosyst.* 2009;5(12):1512–26.
36. Koussounadis A, Langdon SP, Um IH, Harrison DJ, Smith VA. Relationship between differentially expressed mRNA and mRNA-protein correlations in a xenograft model system. *Sci Rep.* 2015;5:10775.
37. Pateras IS, Apostolopoulou K, Niforou K, Kotsinas A, Gorgoulis VG. p57KIP2: “KIP”ing the cell under control. *Mol Cancer Res.* 2009;7(12):1902–19.
38. Mancini-DiNardo D, Steele SJ, Ingram RS, Tilghman SM. A differentially methylated region within the gene Kcnq1 functions as an imprinted promoter and silencer. *Hum Mol Genet.* 2003;12(3):283–94.
39. Li Y, Nagai H, Ohno T, Yuge M, Hatano S, Ito E, Mori N, Saito H, Kinoshita T. Aberrant DNA methylation of p57(KIP2) gene in the promoter region in lymphoid malignancies of B-cell phenotype. *Blood.* 2002;100(7):2572–7.
40. Shen L, Toyota M, Kondo Y, Obata T, Daniel S, Pierce S, Imai K, Kantarjian HM, Issa JP, Garcia-Manero G. Aberrant DNA methylation of p57KIP2 identifies a cell-cycle regulatory pathway with prognostic impact in adult acute lymphocytic leukemia. *Blood.* 2003;101(10):4131–6.
41. Kikuchi T, Toyota M, Itoh F, Suzuki H, Obata T, Yamamoto H, Kakiuchi H, Kusano M, Issa JP, Tokino T, et al. Inactivation of p57KIP2 by regional promoter hypermethylation and histone deacetylation in human tumors. *Oncogene.* 2002;21(17):2741–9.
42. Yang X, Karuturi RK, Sun F, Au M, Yu K, Shao R, Miller LD, Tan PB, Yu Q. CDKN1C (p57) is a direct target of EZH2 and suppressed by multiple epigenetic mechanisms in breast cancer cells. *PLoS One.* 2009;4(4):e5011.
43. Fornari F, Gramantieri L, Ferracin M, Veronese A, Sabbioni S, Calin GA, Grazi GL, Giovannini C, Croce CM, Bolondi L, et al. MiR-221 controls CDKN1C/p57 and CDKN1B/p27 expression in human hepatocellular carcinoma. *Oncogene.* 2008;27(43):5651–61.
44. Pulikkan JA, Dengler V, Peramangalam PS, Peer Zada AA, Muller-Tidow C, Bohlander SK, Tenen DG, Behre G. Cell-cycle regulator E2F1 and microRNA-223 comprise an autoregulatory negative feedback loop in acute myeloid leukemia. *Blood.* 2010;115(9):1768–78.
45. Kim YK, Yu J, Han TS, Park SY, Namkoong B, Kim DH, Hur K, Yoo MW, Lee HJ, Yang HK, et al. Functional links between clustered microRNAs: suppression of cell-cycle inhibitors by microRNA clusters in gastric cancer. *Nucleic Acids Res.* 2009;37(5):1672–81.
46. Burkhart DL, Sage J. Cellular mechanisms of tumour suppression by the retinoblastoma gene. *Nat Rev Cancer.* 2008;8(9):671–82.
47. Polager S, Ginsberg D. E2F - at the crossroads of life and death. *Trends Cell Biol.* 2008;18(11):528–35.
48. Dar AA, Majid S, de Semir D, Nosrati M, Bezrookove V, Kashani-Sabet M: miRNA-205 suppresses melanoma cell proliferation and induces senescence via regulation of E2F1 protein. *J Biol Chem.* 2011;286(19):16606–14.
49. Bourdon JC, Fernandes K, Murray-Zmijewski F, Liu G, Diot A, Xirodimas DP, Saville MK, Lane DP. p53 isoforms can regulate p53 transcriptional activity. *Genes Dev.* 2005;19(18):2122–37.
50. Aoubala M, Murray-Zmijewski F, Khoury MP, Fernandes K, Perrier S, Bernard H, Prats AC, Lane DP, Bourdon JC. p53 directly transactivates Delta133p53alpha, regulating cell fate outcome in response to DNA damage. *Cell Death Differ.* 2011;18(2):248–58.
51. Olivier M, Petitjean A, Marcel V, Petre A, Mounawar M, Plymoth A, de Fromental CC, Hainaut P. Recent advances in p53 research: an interdisciplinary perspective. *Cancer Gene Ther.* 2009;16(1):1–12.
52. Brooks LA, Tidy JA, Gusterson B, Hiller L, O’Nions J, Gasco M, Marin MC, Farrell PJ, Kaelin WG Jr, Crook T. Preferential retention of codon 72 arginine p53 in squamous cell carcinomas of the vulva occurs in cancers positive and negative for human papillomavirus. *Cancer Res.* 2000;60(24):6875–7.
53. Schneider-Stock R, Mawrin C, Motsch C, Boltze C, Peters B, Hartig R, Buhtz P, Giers A, Rohrbeck A, Freigang B, et al. Retention of the arginine allele in codon 72 of the p53 gene correlates with poor apoptosis in head and neck cancer. *Am J Pathol.* 2004;164(4):1233–41.
54. Kawaguchi H, Ohno S, Araki K, Miyazaki M, Saeki H, Watanabe M, Tanaka S, Sugimachi K. p53 polymorphism in human papillomavirus-associated esophageal cancer. *Cancer Res.* 2000;60(11):2753–5.
55. Schneider-Stock R, Boltze C, Peters B, Szibor R, Landt O, Meyer F, Roessner A. Selective loss of codon 72 proline p53 and frequent mutational inactivation of the retained arginine allele in colorectal cancer. *Neoplasia.* 2004;6(5):529–35.
56. Furihata M, Takeuchi T, Matsumoto M, Kurabayashi A, Ohtsuki Y, Terao N, Kuwahara M, Shuin T. p53 mutation arising in Arg72 allele in the tumorigenesis and development of carcinoma of the urinary tract. *Clin Cancer Res.* 2002;8(5):1192–5.
57. Papadakis ED, Soultz N, Spandidos DA. Association of p53 codon 72 polymorphism with advanced lung cancer: the Arg allele is preferentially retained in tumours arising in Arg/pro germline heterozygotes. *Br J Cancer.* 2002;87(9):1013–8.
58. Soultz N, Sourvinos G, Dokianakis DN, Spandidos DA. p53 codon 72 polymorphism and its association with bladder cancer. *Cancer Lett.* 2002; 179(2):175–83.